

Magnetism of Cuprate Oxides

G. Shirane

Brookhaven National Laboratory, Upton, NY 11973, USA

Abstract

A review is given of the current neutron scattering experiments on cuprate oxides. We first discuss the extensive neutron measurements on high T_c oxides; $\text{La}_{2-x}\text{Sr}_x\text{CuO}_4$ and related $\text{La}_{1.6-x}\text{Nd}_{0.4}\text{Sr}_x\text{CuO}_4$. The second topic is the spin-Peierls system $\text{Cu}_{1-x}\text{Zn}_x\text{GeO}_3$, where a new type of antiferromagnetic phase has been discovered.

1 Introduction

It has been ten years since the discovery of high T_c superconductors by Bednorz and Müller (1986). Very extensive neutron scattering studies have been carried out both on $\text{La}_{2-x}\text{Sr}_x\text{CuO}_4$ (214-type) and $\text{YBa}_2\text{Cu}_3\text{O}_{6+d}$ (123-type). In this review, we limit our discussions only to the 214 type oxides and report some of the recent advances by the neutron scattering techniques.

The high T_c discovery prompted an extensive search for other copper oxides for new compounds of superconductivity. This resulted in opening a new field of magnetism not directly related to superconductivity. One of the most interesting copper oxides in this category is the spin-Peierls oxide CuGeO_3 , discovered by Hase et al. (1993). This oxide goes into the singlet dimer state below $T_{\text{sp}} = 14$ K and is the first example of a simple oxide exhibiting a spin-Peierls transition. Again, the doping of Cu or Ge reveals very interesting phenomena, just like the doping of the high T_c oxides.

2 High T_c oxides: $\text{La}_{2-x}\text{Sr}_x\text{CuO}_4$ type

The antiferromagnetic spin fluctuations in these copper oxides have been studied extensively and a review was given by Shirane et al. (1994). The double peaks in q scan across the 2D ridge was first reported by Birgeneau et al. (1989) and the exact locations of satellite peaks were later mapped out by Cheong et al. (1991). Despite extensive neutron scattering studies of $\text{La}_{1.85}\text{Sr}_{0.15}\text{CuO}_4$, the existence of energy

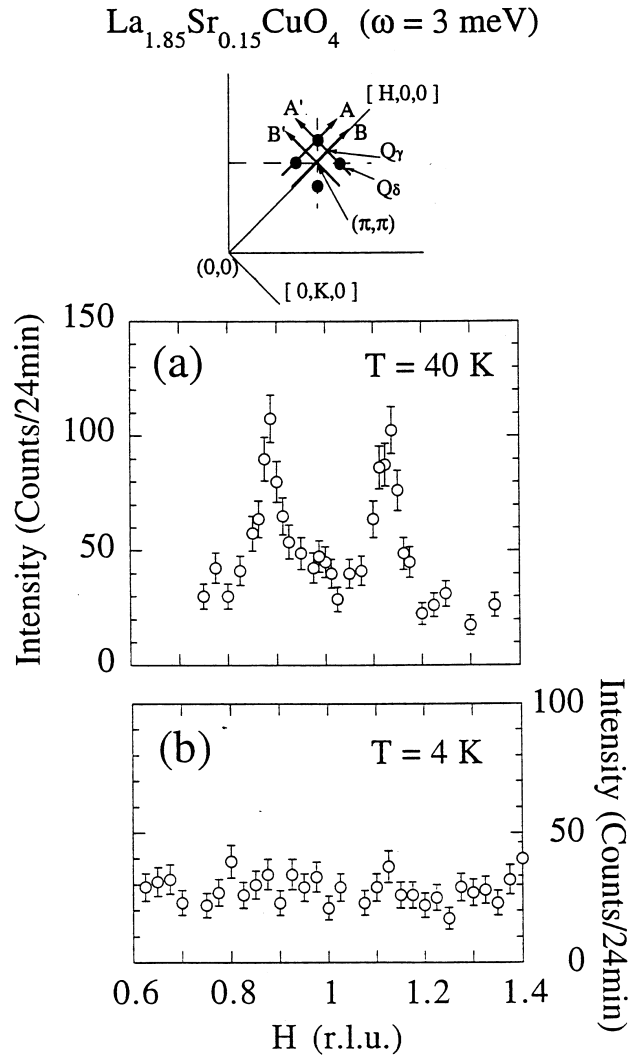


Figure 1. Neutron inelastic scattering spectra at 3 meV for Sendai crystal 1 at $T = 40$ K ($> T_c$) (a) and $T = 4$ K (b) taken by scan A. At the top is a schematic drawing of reciprocal space near the (π, π) position; typical scan directions are denoted by A, A', B, and B'. The closed circles denote the peak positions of the incommensurate magnetic fluctuations. In the $[HHL]$ zone, scans A and B can be performed with tilts of the crystal around the c^* axis equal to 6° and 10° , respectively. After Yamada et al. (1995).

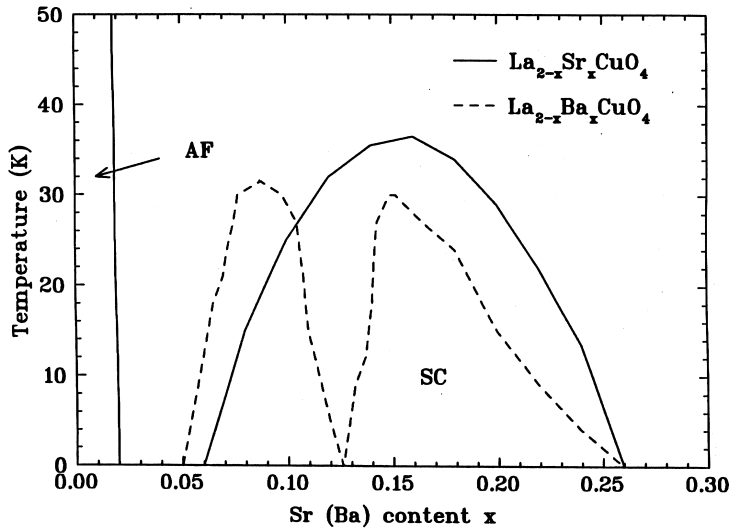


Figure 2. Phase diagram of $\text{La}_{2-x}\text{Sr}_x\text{CuO}_4$ (solid line). AF denotes antiferromagnetic order and SC indicates superconductivity. Dashed line indicates the superconducting regime in $\text{La}_{2-x}\text{Ba}_x\text{CuO}_4$.

gap in magnetic excitation spectrum has only been demonstrated very recently (Yamada et al., 1995).

The progress of the neutron scattering study of high T_c oxides has always been dictated by the successful crystal growth of better (and larger) crystals. The latest step along this line for $\text{La}_{1.85}\text{Sr}_{0.15}\text{CuO}_4$ was accomplished by Hosoya et al. (1994). These crystals are called Sendai, where they were grown, and they show the highest onset of T_c at 37.3 K. Improved quality of the crystals is also reflected in the sharp phase transition between orthorhombic and tetragonal phases. Very recently, Yamada et al. (1996) extended the study for a wide range of x in $\text{La}_{2-x}\text{Sr}_x\text{CuO}_4$. These very interesting experimental results are discussed extensively by Y. Endoh in this conference. Thus, we limit ourselves only to the special topics related to the incommensurate peaks around (π, π) position.

The neutron data shown in Fig. 1 were taken with a large (1.5 cm^3) and nearly perfect single crystal. In contrast to the results reported on lower T_c -crystals, the intensity below 3.5 meV dramatically decreases as the temperature decreases below T_c , and vanishes into the background below 15 K. The clear cut gap is observed only at the optimal doping $x = 0.15$ with $\delta = 0.12$. The important relation between $\delta(x)$ and T_c is discussed by Endoh.

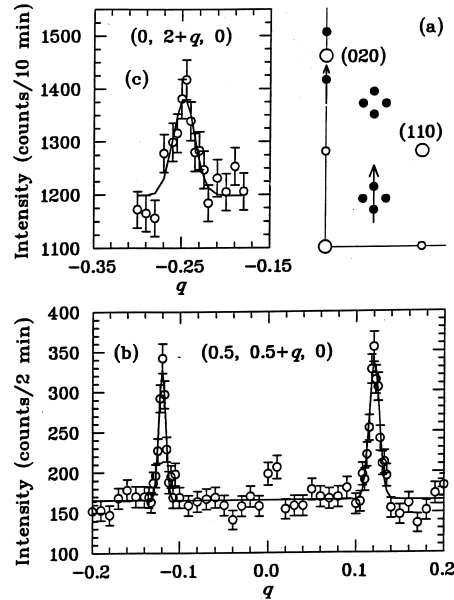


Figure 3. Elastic scans with 2.4 Å neutrons of superlattice peaks consistent with the proposed spin and charge stripes, in $\text{La}_{1.48}\text{Nd}_{0.4}\text{Sr}_{0.12}\text{CuO}_4$ at 11 K. (a) Diagram of the $(h k 0)$ zone of reciprocal space. Open circles indicate locations of Bragg peaks for the LTT structure; solid circles denote spin- and charge-ordering superlattice peaks. Arrows indicate the regions scanned. (b) Scan along $(\frac{1}{2}, \frac{1}{2} + q, 0)$ through the $(\frac{1}{2}, \frac{1}{2} \pm \epsilon, 0)$ peaks. The small peak width indicates that the in-plane correlation length is greater than 150. (c) Scan along $(0, 2 + q, 0)$ through the $(0, 2 - 2\epsilon, 0)$ peak. The lines in (b) and (c) are the result of least-squares fits to gaussian peak shapes plus a flat background. After Tranquada et al. (1995).

3 The 1/8 problem

One of the long-standing puzzles in high T_c research is depicted in Fig. 2. An amazing dip of T_c vs. composition in $\text{La}_{2-x}\text{Ba}_x\text{CuO}_4$ was discovered by Moodenbaugh et al. (1988). Axe et al. (1989) then demonstrated that this dip is related to the phase transition from the low temperature orthorhombic (LTO) to low temperature tetragonal (LTT) structure. It is not possible to grow large enough single crystals of $\text{La}_{2-x}\text{Ba}_x\text{CuO}_4$ to study this feature, but crystals are available for $\text{La}_{2-x-y}\text{Nd}_y\text{Sr}_x\text{O}_4$, which exhibits a similar dip in T_c as a function of x . This is called the 1/8 problem because the dip in T_c (see Fig. 2) corresponds to the x value of 1/8.

Very recently Tranquada et al. (1995) have carried out an elegant and com-

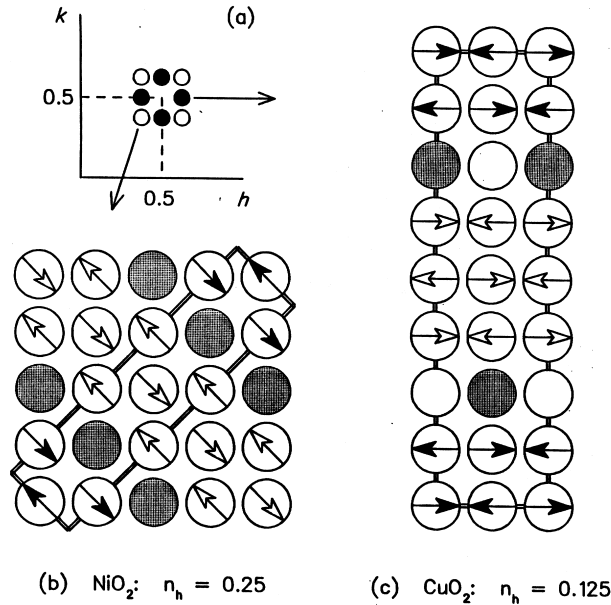


Figure 4. (a) Sketch of the $(hk0)$ zone of the reciprocal lattice showing the positions of the magnetic scattering peaks observed for hole-doped La_2CuO_4 (filled circles) and La_2NiO_4 (open circles). (b) Idealized diagram of the spin and charge stripe pattern within an NiO_2 plane observed in hole-doped La_2CuO_4 with $n_h = 1/4$. (c) Proposed stripe pattern in a CuO_2 plane of hole-doped La_2CuO_4 with $n_h = 1/8$. In both (b) and (c), only the metal atoms are represented; the oxygen atoms, which surround the metal sites in a square planar array, have been left out. After Tranquada et al. (1995).

prehensive neutron scattering experiments on $\text{La}_{1.48}\text{Nd}_{0.4}\text{Sr}_{0.12}\text{CuO}_4$. Their key results are shown in Fig. 3, which also depicts the scattering geometry. Incommensurate dynamical spin correlations have been known in $\text{La}_{2-x}\text{Sr}_x\text{CuO}_4$ (see Fig. 1) for sometime. What is new in Fig. 3 is that these magnetic peaks at δ are elastic Bragg peaks. Moreover, the 2δ peak is observed around (200) (tetragonal notation), and this represents the charge modulation. The LTT structure plays the key role for this special type of stripe phase (see Fig. 4).

This development of the charge density wave (CDW) is the cause of depression of T_c . The phase transition from LTO to LTT phase occurs at 70 K. The transition to the CDW phase takes place around 60 K, which is 10 K higher than the magnetic transition near 50 K. In this system, the phase transition is driven by charge and it is quite different from the case of Cr when the charge part is the secondary effect of the spin ordering. Further study of these fascinating phase transitions continues.

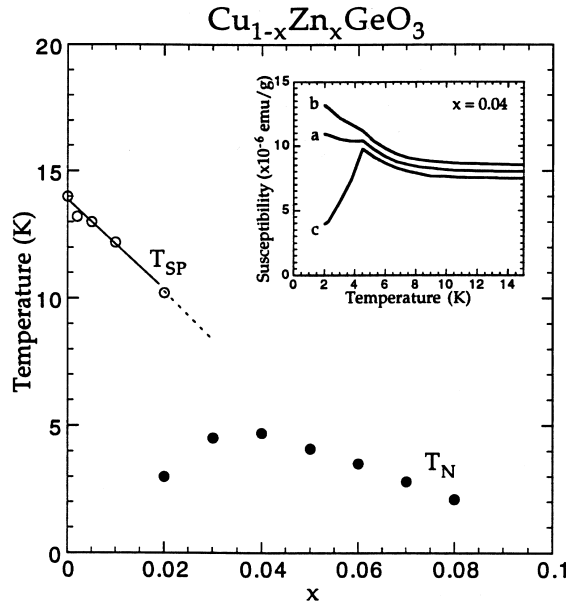


Figure 5. The previously reported phase diagram for $\text{Cu}_{1-x}\text{Zn}_x\text{GeO}_3$ as deduced from magnetic susceptibility measurements of powders. The inset shows the susceptibility measurement of an $x = 0.04$ single crystal in the a , b and c crystallographic directions as labeled. After Hase et al. (1993, 1995).

4 Doped spin-Peierls system $\text{Cu}(\text{Zn})\text{GeO}_3$

The spin-Peierls (SP) transition in CuGeO_3 at $T_{\text{sp}} = 14$ K was discovered by Hase et al. (1993). Previous examples of spin-Peierls systems were all organic compounds and this simple inorganic oxide, gives us the first chance for full understanding of the detailed mechanism of the phase transition into a singlet state mainly because large single crystals can be produced. Comprehensive measurements have already been carried out on important physical properties of CuGeO_3 ; energy gap and magnetic excitations by Nishi et al. (1994) dimerized atomic configuration by Hirota et al. (1994). The structure below 14 K is the simple combined displacements of coppers and oxygen to form alternate dimers in the crystal.

Immediately after the discovery of CuGeO_3 , the effect of substitution of Zn for Cu was reported by Hase et al. (1993). Then followed several papers on $\text{Cu}(\text{Zn})$ and $\text{Ge}(\text{Si})$ doping. I shall discuss in some detail our current neutron scattering studies at Brookhaven on Zn doped CuGeO_3 . This topic may be somewhat out of place for a conference on Magnetism in “Metals”, but the coexistence of antiferromagnetic

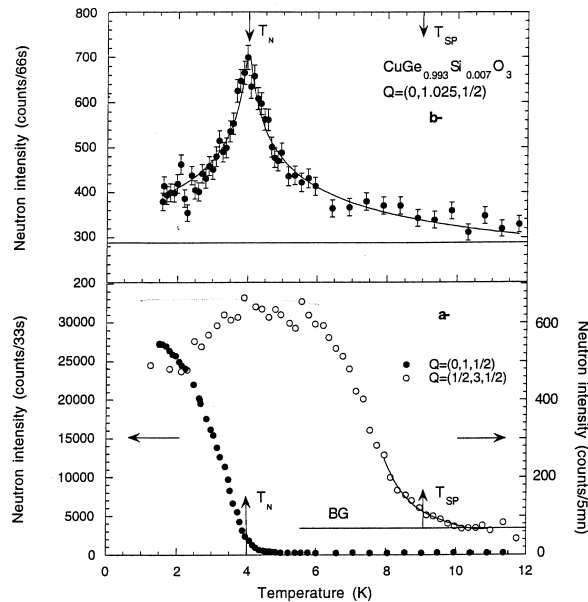


Figure 6. Temperature dependencies of elastic contributions at scattering vectors (a) $\mathbf{Q} = (\frac{1}{2}, 3, \frac{1}{2})$ and $\mathbf{Q} = (0, 1, \frac{1}{2})$ and (b) $\mathbf{Q} = (0, 1.025, \frac{1}{2})$, showing the occurrence of an antiferromagnetic phase transition at $T_N = 4$ K. After Regnault et al. (1995).

(AF) order with spin-Peierls dimerization is a new and exciting physics, which may have future implications on other branches of magnetism and phase transitions. From measurements on powder samples, it is now well established that a new AF ordered phase appears as shown in the phase diagram of Fig. 5. The SP transition is near 14.2 K for the undoped oxide, decreases in temperature with increased Zn concentration, and seemed to disappear around 2% Zn. At 4% Zn, the magnetic susceptibility no longer shows a SP transition, but only a Néel temperature $T_N \sim 4$ K.

A very surprising result was then reported by Regnault et al. (1995) in their neutron scattering study of 0.7% Si-doped CuGeO_3 . As shown in Fig. 6 Regnault et al. demonstrated the successive SP (9 K) and AF (4 K) transitions with two separate branches of magnetic excitations below T_N . Note that the dimer peak $(\frac{1}{2}, 3, \frac{1}{2})$ decreases below T_N but does not disappear. The co-existence of the SP and AF state was first demonstrated in this work. The coexistence of two order parameters, in this fashion, is extremely rare in structural and magnetic phase transitions.

The phase diagram of doped $\text{Cu}(\text{Zn})\text{GeO}_3$, was re-examined by Sasago et al.

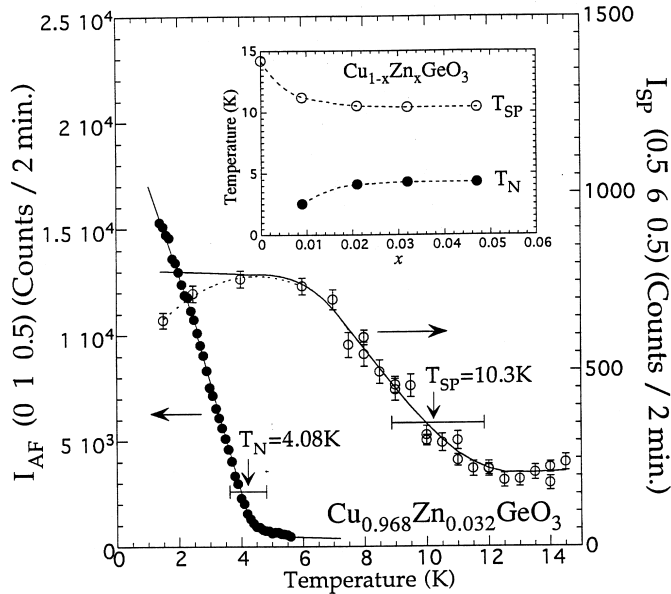


Figure 7. Intensities of the SP and AF superlattice peaks as functions of temperature for a 3.2% Zn-doped crystal. The intensity of the SP lattice dimerization peak is seen to decrease below T_N , however the states are clearly coexisting. The inset shows T_{SP} and T_N measured on samples of 0, 0.9, 2.1, 3.2, and 4.7% Zn-doped crystals. After Sasago et al. (1996).

(1996) and, as shown in Fig. 7, the co-existence of AF and SP phases is also demonstrated in this system. As shown in the inset of Fig. 5, the T_{SP} at 10 K in the 4% Zn sample does not reveal itself in the magnetic susceptibility measurement. However, this is clearly seen in neutron scattering by the appearance of the dimer line ($\frac{1}{2}$ 6 $\frac{1}{2}$) in Fig. 7.

The SP transition persists up to nearly 5% Zn concentration. Fukuyama et al. (1996) proposed a theoretical model for antiferromagnetic order in disordered spin-Peierls systems. They suggest that, surprisingly, long range lattice distortions will actually enhance the degree of the long range coherence of the antiferromagnetism. This model is quite different from the conventional “percolation” type idea in which islands of activated AF copper moments around Zn dopants eventually form “connected” AF order. Fukuyama et al. proposes explicit shape of both order parameters (Cu moment and dimer shift) as a function of dopant concentration. A particularly intriguing question is the lowest limit of concentration x for the appearance of the AF phase. This problem is now being pursued by Martin et al.

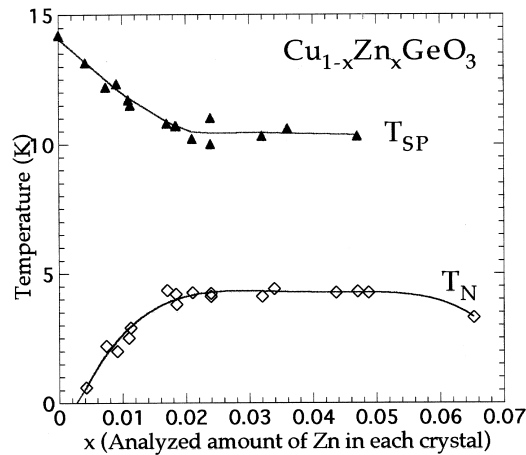


Figure 8. The current phase diagram of $\text{Cu}(\text{Zn})\text{GeO}_3$ constructed by Martin et al. (1996) for neutron and susceptibility measurements.

(1996). They recently observed a long range AF peak below 0.6 K for Zn concentration of 0.4%. It is rather unbelievable that such a small concentration of Zn substitution does create true long range magnetic order. The phase diagram of the $\text{Cu}_{1-x}\text{Zn}_x\text{GeO}_3$ system is constructed by Martin et al. (1996) and shown in Fig. 8. The data combined both neutron and susceptibility measurements. How about the magnetic excitations? Regnault et al. (1995) reported the existence of separate low energy extensions in small q regions from AF peak $(0\ 1\ \frac{1}{2})$. Extensive neutron scattering measurements are now being carried out by Martin et al. (1996) and they have extended AF mode measurements to much wider range in q space. Further neutron scattering studies are needed to complete the picture of this fascinating system.

Acknowledgements

I would like to thank my collaborators for the stimulating discussions, in particular, R.J. Birgeneau, Y. Endoh, V.J. Emery, H. Fukuyama, M. Hase, K. Hirota, Y. Sasago, J.M. Tranquada, K. Uchinokura, and K. Yamada. This work was supported in part by the U.S. Japan collaboration on Neutron Scattering and NEDO International Research grant. Research at Brookhaven was carried out under contract No. DE-AC02-76CH00016, Division of Materials Science, U.S. Department of Energy.

References

- Axe JD, Moudden AH, Holwein D, Cox DE, Mohanty KM, Moodenbaugh A, Yu Y, 1989: *Phys. Rev. Lett.* **62**, 2751
- Bednorz JG, and Müller KA, 1986: *Z. Phys. B* **64**, 189
- Birgeneau RJ, Endoh Y, Hidaka Y, Kakurai K, Kastner MA, Murakami T, Shirane G, Thurston TR and Yamada K, 1989: *Phys. Rev. B* **39**, 2868
- Cheong S-W, Aeppli G, Mason TE, Mook HA, Hayden SM, Canfield PC, Fisk Z, Clausen KN and Kojima H, 1991 (unpublished)
- Fukuyama H, Tanimoto T and Saito M, 1996: *J. Phys. Soc. Jpn.* **65**, 1182
- Hase M, Terasaki I, Uchinokura K, 1993a: *Phys. Rev. Lett.* **70**, 3651
- Hase M, Terasaki I, Sasago Y, Uchinokura K and Obara H, 1993b: *Phys. Rev. Lett.* **71**, 4059
- Hase M, Uchinokura K, Birgeneau RJ, Hirota K and Shirane G, 1996: *J. Phys. Soc. Jpn.* **65**, 1392
- Hirota K, Cox DE, Lorenzo JE, Shirane G, Tranquada JM, Hase M, Uchinokura K, Kojima H, Shibuya Y and Tanaka I, 1994: *Phys. Rev. Lett.* **73**, 736
- Hosoya S, Lee CH, Wakimoto S, Yamada K and Endoh Y, 1994: *Physica C* **235**, 547
- Martin M, Hase M, Hirota K, Shirane G, Sasago Y, Koide N and Uchinokura 1996: (unpublished)
- Moodenbaugh AR, Xu Y, Suenaga M, Folkerts TJ and Shelton RN, 1988: *Phys. Rev. B* **38**, 4596
- Nishi M, Fujita O and Akimitsu J, 1994: *Phys. Rev. B* **50**, 6508
- Regnault LP, Renard JP, Dhalenne G and Revcolevschi A, 1995: *Europhys. Lett.* **32**, 579
- Sasago Y, Koide N, Uchinokura K, Martin MC, Hase M, Hirota K and Shirane G, 1996: *Phys. Rev. B* (to be published)
- Shirane G, Birgeneau RJ, Endoh Y, Kastner MA, 1994: *Physica B* **197**, 158
- Tranquada JM, Sternlieb BJ, Axe JD, Nakamura Y and Uchida S, 1995: *Nature* **375**, 561
- Yamada K, Wakimoto S, Shirane G, Lee CH, Kastner MA, Hosoya S, Greven J, Endoh Y and Birgeneau RJ, 1995: *Phys. Rev. Lett.* **75**, 1626
- Yamada K, Wada J, Kurahashi K, Lee CH, Kimura Y, Wakimoto S, Endoh Y, Hosoya S, Shirane G, Birgeneau RJ and Kastner MA, 1996: (submitted)